Journal of Physics: Conference Series **736** (2016) 012014 doi:10.1088/1742-6596/736/1/012014

PHENIX results on collectivity in high-multiplicity p + Au, d + Au and ^{3}He + Au collisions

Qiao Xu, (for the PHENIX Collaboration)
Physics and Astronomy Department, Vanderbilt University, U.S.A
E-mail: qiao.xu@vanderbilt.edu

Abstract. We present recent PHENIX results for long-range two-particle correlation functions across a large pseudorapidity(η) gap in high-multiplicity p+Au, d+Au and ^{3}He+Au collisions. Enhanced correlations are observed for particles with small azimuthal separation. Measurements of the second order Fourier coefficients (v_2) in p/d/^{3}He+Au collisions, and the third order Fourier coefficient (v_3) in ^{3}He+Au collision are performed using the event plane method. Scaling of v_2 with the initial eccentricity (ε_2) is performed in each system to investigate the role of the initial geometry in the development of a final-state anisotropy in the particle emission. The v_2 coefficients for identified $\pi^{\pm}$, $K^{\pm}$ and (anti-)proton are measured as a function of transverse kinetic energy (KE_T) and their magnitudes are found to scale approximately with the number of constituent quarks in the hadron.

Introduction

Collective flow is one of the defining signatures of quark-gluon plasma (QGP) formation in high-energy nucleus-nucleus (AA) collisions. It has long been considered that a large volume, in which a thermal equilibrium can be achieved, is a prerequisite for QGP formation. However, a number of recent measurements from high-multiplicity collisions in small systems at RHIC [1, 2, 3] and LHC [4, 5, 6, 7] have found strong correlations between the produced particles reminiscent of those observed in the AA collisions. In AA collisions, the final-state particles anisotropies are well described by hydrodynamics models with small specific viscosity. In these models, the anisotropies are driven by the pressure gradients in the initial energy density. There are different initial state models, some of which, such as the IP-glasma model [8], involve gluon saturation. Alternatively, the system evolution can be described on a microscopic level with partonic and hadronic scatterings, such as in the AMPT model [9]. These models have different sensitivity to the initial geometry in the collisions [10]. To investigate if QGP can be formed in small system, and if the observed correlations can be attributed to collective hydrodynamic flow, the PHENIX experiment has conducted a series of geometry-controlled experiments using 0-5% central p/d/^{3}He + Au collision at $\sqrt{s_{NN}}$ = 200 GeV. The two-particle correlations and the Fourier coefficients in the single-particle azimuthal distributions are studied as a function of transverse momentum.

1. Experiment Details

In the PHENIX detector [11], charged particle trajectories are reconstructed with the two central arm using the drift chambers (DC) and multi-wire proportional chambers (PC) [11], covering

$|\eta| < 0.35$ and $\pi/2$ in azimuthal angle each. The drift chamber tracks are projected to the third layer of the PC and matched to hits in this detector, to decrease the contribution from mis-reconstructed tracks. Time-of-Flight detectors (TOF) are used for hadron identification. TOF is comprised of two arms: east arm (TOFe) and west arms (TOEw). Identification of $\pi^{\pm}$, $K^{\pm}$ and (anti-)proton in a momentum range up to 3 GeV/c is achieved over 99% purity [12, 13].

The beam-beam counters (BBC) [11] consist two arrays of 64 photomultiplier tubes (PMTs) each, covering 2π in azimuth and $3.1 < |\eta| < 3.9$ in pseudorapidity. The Forward Silicon Vertex Detector (FVTX) consists of two identical end-cap assemblies, covering $1.0 < |\eta| < 3.0$. The event planes are measured in the Au-going direction using the charge deposited in the south BBC (BBC-S), as well as the reconstructed clusters in the south end-cap of FVTX (FVTX-S).

The p+Au, d+Au and ^{3}He+Au data sets were collected in year 2015, 2008, and 2014, respectively. In p+Au and ^{3}He+Au collisions, high multiplicity (HM) triggers were implemented to enrich the central events. The high multiplicity trigger is based on the minimum bias trigger, but imposes additional requirement of more than 48 photomultiplier tubes firing in the BBC-S in p+Au collisions, which corresponds approximately to the 5% most central events. A similar high multiplicity trigger was used on 2014 run for ^{3}He+Au collisions. The HM trigger increases the recorded central event samples, in comparison to the minimum bias sample, by 40 times in p+Au and 10 times in ^{3}He+Au collisions.

Centrality classes are determined as a percentile of the total multiplicity measured in the BBC-S, following the procedure documented in Ref. [14]. In this analysis we select the 0-5% most central events. The initial geometry for the corresponding centrality is computed and characterized by a standard Monte Carlo (MC) Glauber model [15] with a Gaussian smearing of the nucleon distributions with $\sigma = 0.4$ fm.

2. Analysis method

The two-particle azimuthal correlations are measured between tracks in the PHENIX central arm at a given transverse momentum(p_T) and charge measured in the PMTs in the BBC-S, which is on Au-going side. The correlation function is constructed as a function of relative azimuthal angle $\Delta\phi$ and p_T using pairs from the same event $S(\Delta\phi, p_T)$ and normalized to the correlations in mixed events $M(\Delta\phi, p_T)$, where the particles in the pair come from different events, following the same procedure as in [3]:

$$S(\Delta\phi, p_T) = \frac{d(w_{pmt} N_{sameevent}^{Track(p_T)-PMT})}{d\Delta\phi} \tag{1}$$

$$C(\Delta\phi, p_T) = \frac{S(\Delta\phi, p_T)}{M(\Delta\phi, p_T)} \frac{\int M(\Delta\phi', p_T) d\Delta\phi'}{\int S(\Delta\phi', p_T) d\Delta\phi'} \tag{2}$$

where the w_{pmt} is taken from the total charge from the BBC-S PMTs.

We measure the flow coefficient with the event plane method [16].

$$v_n = \frac{< \cos(n(\phi - \Psi_{n,BBC_s}) >}{Res(\Psi_{n,BBC_s})} \tag{3}$$

The event plane is determined by detectors at large pseudorapidity, and the standard re-centering and flattering procedures are applied to calibrate the event-plane distributions [16]. To determine the event plane resolution, the three sub-event method is used:

$$Res(\Psi_{n,BBC_s}) =< \cos(n(\Psi_{n,BBC_s} - \Psi_{RP})) >= \sqrt{\frac{< \cos(n(\Psi_{n,BBC_s} - \Psi_{n,CNT})) >< \cos(n(\Psi_{n,BBC_s} - \Psi_{n,FVTX_s})) >}{< \cos(n(\Psi_{n,CNT} - \Psi_{n,FVTX_s})) >}} \tag{4}$$

Here, $\Psi_{n,CNT}$ is the event plane angle determined by the central arm tracking detectors, Ψ_{n,BBC_s} is the event plane angle determined by the BBC-S PMTs. $\Psi_{n,FVTX_s}$ is the event plane angle determined by the south end-caps of the FVTX.

3. Results

3.1. Correlation function in p+Au, d+Au and ^{3}He+Au collisions

The correlation functions $C(\Delta\phi, p_T)$ for 0-5% central events in p+Au, d+Au and ^{3}He+Au collisions in selected p_T bins, , and compared to the correlation functions measured in minimum bias p+p collisions at the same center-of-mass energy. We analyze these shapes by fitting each correlation function to a four-term Fourier cosine expansion, $f(\Delta\phi) = 1 + \Sigma_{n=1}^{4} c_n(p_T)\cos(n\Delta\phi)$. The fitting results are plotted in Fig. 1 for each distribution. Central ^{3}He+Au and d+Au collisions show a clearly visible enhancement of near-side pairs; central p+Au collisions show a flat distribution in near-side area. In both cases, a sizable second order Fourier term is needed to describe the correlations. In contrast, the p+p collisions can be described almost completely by the dipole term, as expected from back-to-back jets contribution and transverse momentum conservation.

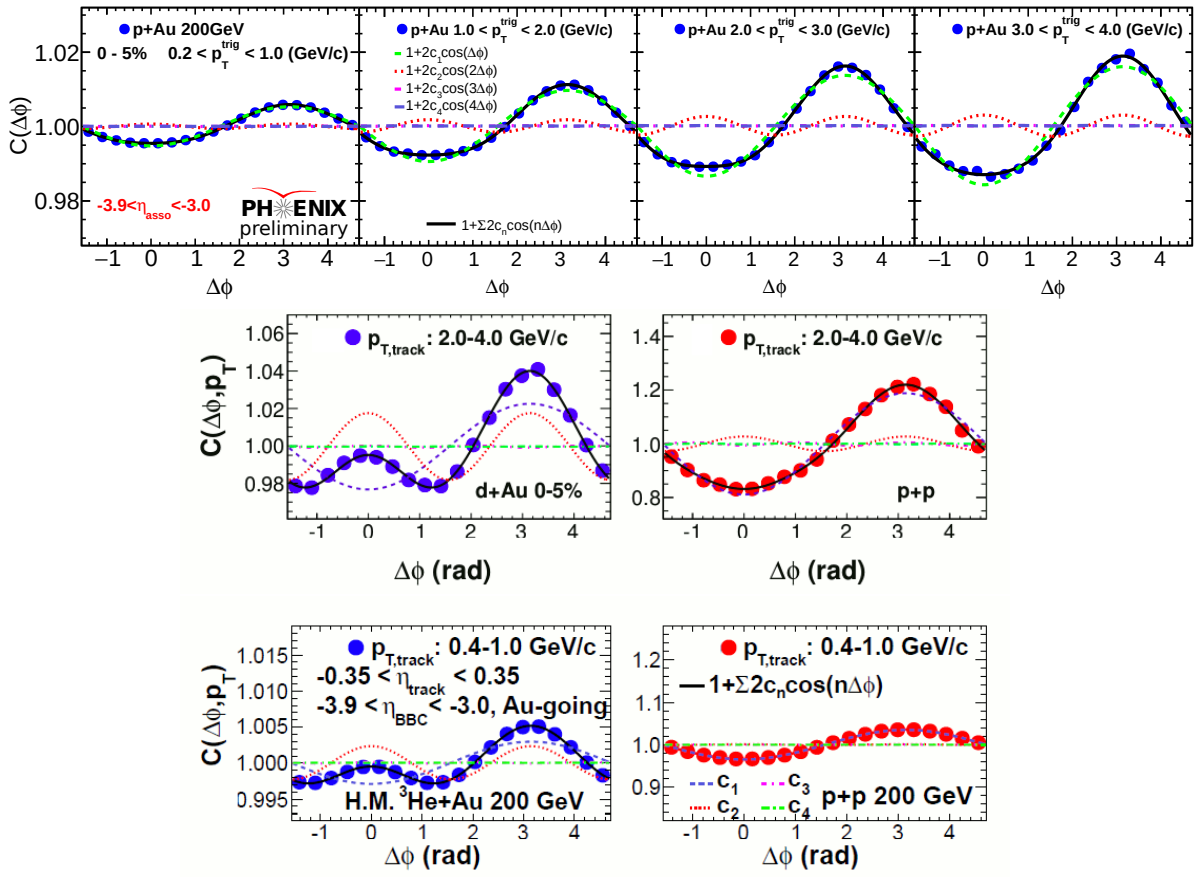

Figure 1. Two-particle correlation functions in high-multiplicity p+Au, d+Au and ^{3}He+Au collisions at $\sqrt{s_{NN}} = 200$ GeV, and comparisons to correlation functions in minimum bias p+p collisions at $\sqrt{s_{NN}} = 200$ GeV.

3.2. Charged hadron v_2 comparison in three systems

To better understand the origin of the near-side peaks and the azimuthal anisotropy in particle production in small system, we compare the v_2 vs p_T in the three systems for 0-5% central event, as shown in Fig. 2. The data clearly indicate that v_2 in p+Au collisions is significant, but smaller than that measured in d+Au [2] and ^{3}He+Au [3]. Given that from Glauber MC, the initial eccentricity ε_2 in central p+Au collisions is smaller than in d+Au and ^{3}He+Au collisions, it supports the hypothesis that the initial geometry plays a major role in determining these anisotropies. The data are compared to the predictions of the SONIC hydrodynamics model [17], which translates the initial state geometry to final-state momentum anisotropies. The SONIC model [17] can describe the data well in all the three systems.

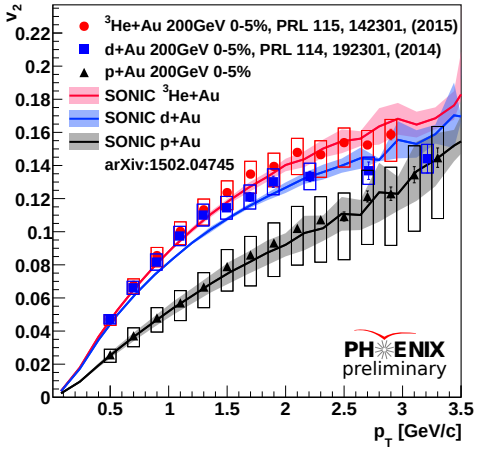

Figure 2. Measured v_2 from 0-5% p/d/^{3}He+Au $\sqrt{s_{NN}}$ = 200 GeV collisions, in comparison to the predictions from the SONIC model [17].

3.3. Charged hadron v_2 and v_3 compared to models

Various models have predicted the anisotropy in small systems with different physics mechanism, including hydrodynamics models with [18] or without pre-flow [17], AMPT model [9], and gluon saturation [8]. In Fig. 3, we compared our results with the predictions of these models. SONIC model[17] and superSONIC [18] predict the v_2 values well in all three systems. Within the current systematics, we cannot tell one from another. AMPT model [9] can predict the three systems up to 1.5 GeV/c. IPGlasma+Hydrodynamic [8] model underpredicts the p+Au results but overpredicts the d/^{3}He+Au results. Clear v_3 signal is observed in central ^{3}He+Au events. The v_3 measured in ^{3}He+Au provides an additional constrain.

3.4. Eccentricity scaling

The quantity v_2/ε_2 is shown in the Fig. 4 in p/d/^{3}He+Au collisions at same energy. The quantity ε_2 of these three systems are from the standard Glauber model calculations[15]. The Glauber model predicts that the initial eccentricity in d+Au collisions is similar to that in ^{3}He+Au collisions but larger than in p+Au collisions. The measured v_2 follows the same order, however, the scaling of the values of v_2 with the corresponding eccentricities in these three system would not collapse to a common pattern. The larger v_2/ε_2 in p+Au collisions may indicate that the substructure of the proton also plays a role.

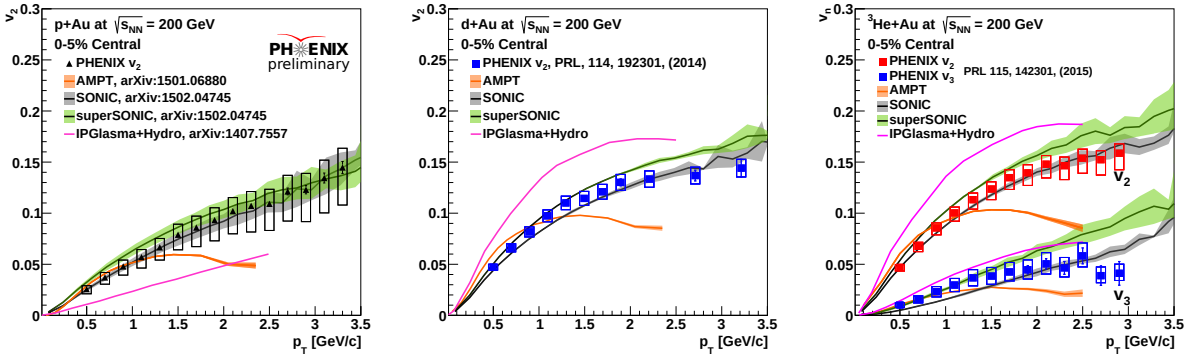

Figure 3. Measured v_2 from 0-5% p/d/^{3}He+Au $\sqrt{s_{NN}}$ = 200 GeV collisions. The data are compared with AMPT, SONIC/superSONIC and IPGlasma models predictions.

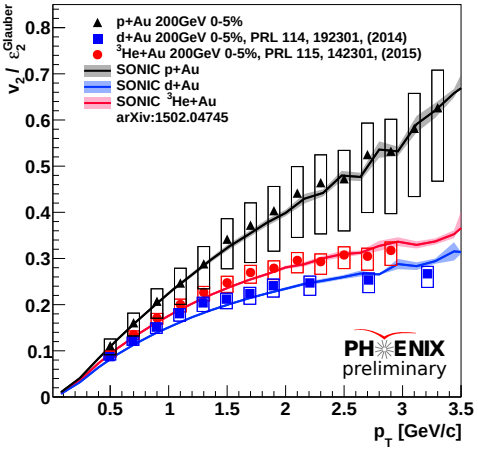

Figure 4. Measured v_2/ε_2 for mid-rapidity for charged tracks in 0-5% central p/d/^{3}He+Au collisions at $\sqrt{s_{NN}}$ = 200 GeV

3.5. Identified particle v_2 in d+Au and ^{3}He+Au collisions

The second order flow coefficients for identified $\pi^{\pm}$, $K^{\pm}$ and (anti-)proton are presented in the left panel of Fig. 5. Mass-ordering is observed in ^{3}He+Au collisions. The trend is consistent with hydrodynamic flow in which the heavier particles are boosted to higher p_T even with same expanding velocity of the medium. The right panel of the Fig. 5 shows that the v_2 values for identified particles can be described by a universal curve when scaled by number of quarks in the hadron. Such scaling previously observed in Au+Au collisions is also seen in the small ^{3}He+Au system, which is consistent with viscous hydro calculations or the quark coalescence models [19, 20].

Conclusions

We have presented measurements of long-range azimuthal correlations between tracks at mid-rapidity $|\eta| < 0.35$, and charges in BBC Au-going direction in p/d/^{3}He+Au collisions at $\sqrt{s_{NN}}$ = 200 GeV. Enhanced correlations with small azimuthal separation are observed for pairs across $|\Delta\eta| > 3.5$ in high multiplicity events. The anisotropic flow coefficients v_2 and v_3 are measured

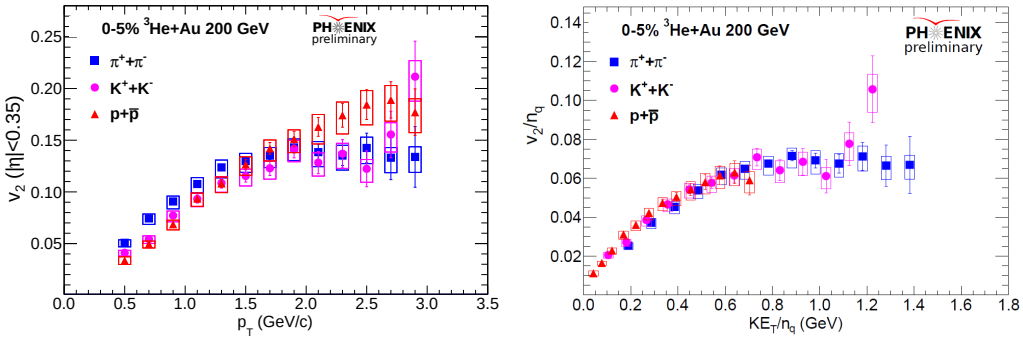

Figure 5. Left panel: Measured v_2 of identified $\pi^{\pm}$, $K^{\pm}$ and (anti-)proton from 0-5% ^{3}He+Au at $\sqrt{s_{NN}}$ = 200 GeV collisions. Right panel: Constituent quark-number (n_q) scaling of v_2 for $\pi^{\pm}$, $K^{\pm}$ and (anti-)proton as a function of transverse kinetic energy $KE_T = \sqrt{p_T^2 + m^2} - m$ in 0-5% central ^{3}He+Au collisions.

for mid-rapidity particles with the event plane method. The v_2 of 0-5% p+Au is sizable and found to be smaller than that of d/^{3}He+Au and indicates that the initial geometry plays an important role in describing system evolution. A sizable v_3 is seen in ^{3}He+Au collisions. Hydrodynamics models with initial conditions from the Glauber model describe v_2 and v_3 quite well. These values of η/s at or near the conjectured lower bound $1/4\pi$ [21] are similar to the ones needed to describe collective flow in large systems, such as Au+Au or Pb+Pb collisions. The measurements of v_2 for identified hadrons in 0-5% ^{3}He+Au collisions are found to scale with the number of quarks, as expected in systems where the flow develops at the partonic level.

References

[1] (PHENIX Collaboration) A. Adare, et al., Quadrupole anisotropy in dihadron azimuthal correlations in central d+Au collisions at $\sqrt{s_{NN}}$ = 200 GeV, Phys. Rev. Lett., 111:212301, Nov 2013.
[2] (PHENIX Collaboration) A. Adare et al., Measurement of long-range angular correlation and quadrupole anisotropy of pions and (anti)protons in central d+Au collisions at $\sqrt{s_{NN}}$ = 200 GeV, Phys. Rev. Lett., 114(19):192301, 2015.
[3] (PHENIX Collaboration) A. Adare et al., Measurements of Elliptic and Triangular Flow in High-Multiplicity ^{3}He+Au Collisions at $\sqrt{s_{NN}}$ = 200 GeV, Phys. Rev. Lett., 115:142301, 2015.
[4] (CMS Collaboration) S. Chatrchyan, et al., Observation of long-range, near-side angular correlations in pPb collisions at the LHC, Phys.Lett. B718 (2013) 795C814.
[5] (ATLAS Collaboration) G. Aad, et al., Observation of Associated Near-Side and Away-Side Long-Range Correlations in $\sqrt{s_{NN}}$ = 5.02 TeV Proton-Lead Collisions with the ATLAS Detector, Phys. Rev. Lett. 110 (2013) 182302.
[6] (ALICE Collaboration) B. Abelev, et al., Long-range angular correlations on the near and away side in p-Pb collisions at $\sqrt{s_{NN}}$ = 5.02 TeV, Phys.Lett. B719 (2013) 29C41.
[7] (CMS Collaboration) S. Chatrchyan, et al., Multiplicity and transverse momentum dependence of two- and four-particle correlations in pPb and PbPb collisions, Phys.Lett. B724 (2013) 213C240.
[8] Bjoern Schenke and Raju Venugopalan, Collective effects in light heavy ion collisions, Nucl. Phys., A931:1039C1044, 2014.
[9] Zi-Wei Lin, Che Ming Ko, Bao-An Li, Bin Zhang, and Subrata Pal. Multiphase transport model for relativistic heavy ion collisions, Phys. Rev. C, 72(6):064901, December 2005.
[10] J. L. Nagle, A. Adare, S. Beckman, T. Koblesky, J. O. Koop, D. McGlinchey, P. Romatschke, J. Carlson, J. E. Lynn, M McCumber, Exploiting Intrinsic Triangular Geometry in Relativistic 3He+Au Collisions to Disentangle Medium Properties, Phys. Rev. Lett. 113 (11) (2014) 112301. doi:10.1103/PhysRevLett.113.112301.
[11] (PHENIX Collaboration) K. Adcox, et al., PHENIX detector overview, Nucl. Instrum. Meth. A499 (2003) 469C479. doi:10.1016/S0168-9002(02)01950-2.

[12] (PHENIX collaboration)Adare, A. et al., Spectra and ratios of identified particles in Au+Au and d+Au collisions at $\sqrt{s_{NN}} = 200$ GeV, Phys. Rev. C 88 (2013) 024906.
[13] (PHENIX collaboration)Adare, A. et al., Deviation from quark number scaling of the anisotropy parameter v_2 of pions, kaons, and protons in Au+Au collisions at $\sqrt{s_{NN}} = 200$ GeV, Phys. Rev. C 85 (2012) 064914.
[14] (PHENIX Collaboration) A. Adare et al., Centrality categorization for Rp(d)+A in high-energy collisions, Phys. Rev. C 90, 034902.
[15] M. L. Miller, K. Reygers, S. J. Sanders, and P. Steinberg, Ann.Rev.Nucl.Part.Sci. 57, 205 (2007), nucl-ex/0701025.
[16] A. M. Poskanzer, S. A. Voloshin, Methods for analyzing anisotropic flow in relativistic nuclear collisions, Phys. Rev. C58 (1998) 1671C1678.
[17] M. Habich, J. L. Nagle, and P. Romatschke, Particle spectra and HBT radii for simulated central nuclear collisions of C + C, Al + Al, Cu + Cu, Au + Au, and Pb + Pb from s = 62.4 - 2760 GeV, Eur. Phys. J., C75(1):15, 2015.
[18] Paul Romatschke. Light-Heavy Ion Collisions: A window into pre-equilibrium QCD dynamics?, Eur. Phys. J., C75(7):305, 2015.
[19] R. C. Hwa, C. B. Yang, Scaling behavior at high p_T and the p/pi ratio, Phys. Rev. C67 (2003) 034902. doi:10.1103/PhysRevC.67.034902.
[20] R. J. Fries, B. Muller, C. Nonaka, S. A. Bass, Hadronization in heavy ion collisions: Recombination and fragmentation of partons, Phys. Rev. Lett. 90 (2003) 202303. doi:10.1103/PhysRevLett.90.202303.
[21] P. K. Kovtun, D. T. Son, and A. O., StarinetsViscosity in Strongly Interacting Quantum Field Theories from Black Hole Physics, Phys. Rev. Lett. 94, 111601.